Tandem Hairpin Motif for Recognition in the Minor Groove of DNA by Pyrrole–Imidazole Polyamides

David M. Herman, Eldon E. Baird, and Peter B. Dervan*[a]

Abstract: Two six-ring hairpin polyamides linked tail-to-turn by a five-carbon tether recognize a predetermined 11-base-pair (bp) site in the minor groove of DNA. Polyamide subunits, containing three pyrrole (Py) or imidazole (Im) aromatic amino acids covalently linked by a turn-specific γ-aminobutyric acid (γ-turn) residue, form six-ring hairpin structures that recognize designated five-base-pair sequences. Replacement of the γ-turn residue with (*R*)-2,4,-diaminobutyric acid [$(R)^{H_2N}\gamma$] provides for enhanced hairpin-DNA-binding affinity and sequence specificty. In order to extend the targetable binding-site size of the hairpin motif, two tandem hairpin polyamides, ImPyPy-(*R*)[ImPyPy-$(R)^{H_2N}\gamma$PyPyPyβ]$^{HN}\gamma$PyPy-PyβDp (**1**) and ImPyPy-(*R*)[ImPyPy-$(R)^{H_2N}\gamma$PyPyPyδ]$^{HN}\gamma$PyPyPyβDp (**2**), were designed such that the carboxy tail of one six-ring hairpin is covalently tethered to the $(R)^{H_2N}\gamma$-turn of the second through β-alanine (β) or 5-aminovaleric acid (δ), respectively. The DNA-binding affinity of each polyamide was characterized by quantitative footprint titration experiments on DNA fragments containing 10-, 11-, or 12-bp match and mismatch sequences. The parent six-ring hairpin ImPyPy-$(R)^{H_2N}\gamma$-PyPyPy-β-Dp binds to a 5-bp 5′-TGTTA-3′ half site with an equilibrium association constant (K_a) = $5 \times 10^9\,M^{-1}$ and 100-fold specificity versus a 5′-TGT**C**A-3′ mismatch site. The tandem-hairpin polyamide **2**, linked by valeric acid, binds the 11-bp site 5′-TGTTATTGTTA-3′ (individual 6-ring hairpin target sites underlined) with $K_a \geqslant 1 \times 10^{12}\,M^{-1}$ and $\geqslant$4500-fold specificity versus the double mismatch sequence 5′-TGT**C**ATTGT**C**A-3′. The 10-bp and 12-bp sites 5′-TGTTATGTTA-3′ and 5′-TGTTATTTGTTA-3′ are bound with at least 70 and 1000-fold reduced affinity, respectively. β- linked polyamide **1** binds to both the 10- and 11-bp sites with $K_a = 2 \times 10^{10}\,M^{-1}$ and to the 12-bp site with $K_a = 9 \times 10^8\,M^{-1}$. The results presented here identify structure elements that expand polyamide-binding-site size by linking previously described hairpin recognition units. Remarkably, a simple aliphatic 5-carbon tether is sufficient to provide increased binding affinity without comprimising hairpin sequence-selectivity.

Keywords: DNA recognition · hydrogen bonds · pairing code · sequence specificity

Introduction

Small synthetic ligands that target predetermined DNA sequences have the potential to control gene expression.[1] Polyamides containing the three aromatic amino acids 3-hydroxypyrrole (Hp), imidazole (Im), and pyrrole (Py) are small molecules that have an affinity and specificity for DNA comparable with naturally occurring DNA binding proteins.[2, 3] DNA recognition depends on a code of side-by-side aromatic amino acid pairings that are oriented N–C with respect to the 5′-3′ direction of the DNA helix in the minor groove.[2–11] An antiparallel pairing of Im opposite Py (Im/Py pair) distinguishes G·C from C·G and both of these from A·T/T·A base pairs (bp).[4] A Py/Py pair binds both A·T and T·A in preference to G·C/C·G.[4, 5] The discrimination of T·A from A·T by means of Hp/Py pairs completes the four base pair code.[3] Eight-ring polyamides have been shown to be cell permeable and to inhibit transcription of a specific gene in cell culture.[1] This provides impetus to develop an ensemble of motifs that recognize a broad binding-site size repertoire.[2–11] It is particularly important to identify ligand–structure elements that amplify existing recognition motifs for binding to DNA sequences 10–16 bp in size.

Hairpin polyamide: A hairpin polyamide motif with γ-aminobutyric acid (γ) serving as a turn-specific internal-guide residue provides specific binding to designated target sites with >100-fold enhanced affinity relative to the unlinked subunits.[9] Studies of polyamide site size limitations suggest that beyond five consecutive rings, the ligand curvature fails to match the pitch of the DNA helix, disrupting the hydrogen bonds and van der Waals interactions responsible for specific

[a] Prof. P. B. Dervan, D. M. Herman, E. E. Baird
Arnold and Mabel Beckman Laboratories of Chemical Synthesis
California Institute of Technology, Pasadena, CA 91125 (USA)
Fax: (+1) 626-568-8824
E-mail: dervan@cco.caltech.edu

  0947-6539/99/0503-0975 $ 17.50+.50/0

polyamide-DNA complex formation.[6, 7a] The recognition of seven base pairs by ten-ring hairpin polyamides containing five contiguous ring pairings represents the upper limit in binding-site sizes targetable by the hairpin motif.[2c] Addition of pairings with β-alanine (β) to form, β/β, β/Py, and β/Im pairs has allowed extension of the hairpin motif to 8-bp recognition.[2e] Cooperative-binding extended hairpins provide one motif for expanding the hairpin recognition for targeting 10–bp and 12–bp sites.[2d] An alternative approach to increase the targetable binding-site size of hairpins would be to identify a strategy for covalently linking existing hairpin motifs without compromising DNA-binding and sequence-specificity.

Within the hairpin structure, replacement of the γ-turn residue with (R)-2,4-diaminobutyric acid [$(R)^{H_2N}\gamma$] has recently been shown to enhance hairpin DNA-binding affinity and sequence specificity.[10] The primary turn amino group provides a potential site for covalently connecting two hairpins. In one potential linkage arrangement, the *C* terminus of the first hairpin is coupled to the α-amino group of the γ-turn of the second by an amino-acid linker (Figure 1). To determine preferred binding-site size and linker length effects for tandem hairpins, two 12-ring polyamides, ImPyPy-(R)[ImPyPy-$(R)^{H_2N}\gamma$-PyPyPy-β-]$^{HN}\gamma$-PyPyPy-β-Dp (**1**) and ImPyPy-(R)[ImPyPy-$(R)^{H_2N}\gamma$-PyPyPy-δ-]$^{HN}\gamma$-PyPyPy-β-Dp (**2**; Figure 2), were synthesized and their DNA binding properties determined on a series of DNA fragments containing 10-, 11-, and 12-bp target sites. Polyamides were synthesized by solid-phase methods,[12] and their purity and identity confirmed by ^{1}H NMR spectroscopy, MALDI-TOF MS, and analytical HPLC. An affnity cleaving derivative ImPyPy-(R)[ImPyPy-$(R)^{EDTA}\gamma$-PyPyPy-δ-]$^{HN}\gamma$-PyPyPy-β-Dp (**2-E**) was synthesized in order to confirm a single predicted binding orientation for the tandem hairpin polyamide. We report here the DNA-binding affinity and sequence selectivity of **1** and **2** for the 10, 11, and 12 bp match sites 5′-TGTTATGTTA-3′, 5′-TGTTATTGTTA-3′, and 5′-TGTTATATGTTA-3′ (5-bp hairpin target sites are underlined) and double mismatch sites 5′-TGT**C**ATGT**C**A-3′, 5′-TGT**C**ATTGT**C**A-3′, and 5′-TGT**C**ATATGT**C**A-3′ (mismatched base pairs are bold) respectively. Precise binding-site sizes were determined by MPE · Fe^{II} footprinting,[13] and binding orientation and stoichiometry confirmed by affinity cleaving experiments.[14] Equilibrium association constants (K_a) of the polyamides for respective match and mismatch binding sites were determined by quantitative DNase I footprint titration.[15]

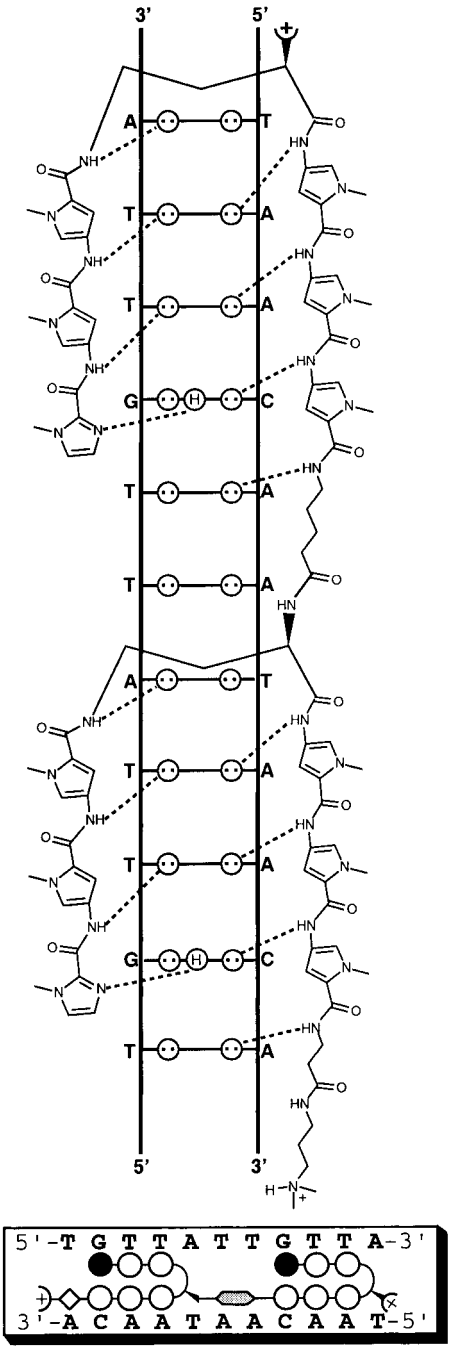

Figure 1. (Top) Hydrogen bonding model of the 1:1 polyamide:DNA complex formed between the tandem hairpin **2** and the 11-bp 5′-TGTTATTGTTA-3′ site. Circles with dots represent lone pairs of N3 of purines and O2 of pyrimidines. Circles containing an H represent the N2 hydrogen of guanine. Putative hydrogen bonds are illustrated by dotted lines. (Bottom) For schematic binding model, Im and Py rings are represented as shaded and unshaded spheres, respectively. The β-residue and valeric acid linker are represented as an unshaded diamond and an unshaded hexagon, respectively.

Results and Discussion

Synthesis: ImPyPy-(R)[ImPyPy-$(R)^{H_2N}\gamma$-PyPyPy-β-]$^{HN}\gamma$-PyPyPy-β-Dp (**1**) and ImPyPy-(R)[ImPyPy-$(R)^{H_2N}\gamma$-PyPyPy-δ-]$^{HN}\gamma$-PyPyPy-β-Dp (**2**) were synthesized from Boc-β-alanine-Pam resin (0.6 g resin, 0.6 mmol g^{-1} substitution) with Boc-chemistry machine-assisted protocols in 31 steps (Figure 3, p. 978).[12] ImPyPy-$(R)^{FmocHN}\gamma$-PyPyPy-β-Pam-Pam resin was prepared as described.[10] The Fmoc protecting group was then removed by treatment with (4:1) piperidine/DMF. The remaining amino acid sequence was then synthesized in a stepwise manner from Boc-chemistry machine-assisted protocols to provide ImPyPy-(R)[ImPyPy-$(R)^{FmocHN}\gamma$-PyPyPy-β-]$^{HN}\gamma$-PyPyPy-β-Pam-Resin and ImPyPy-(R)[ImPyPy-$(R)^{FmocHN}\gamma$-PyPyPy-δ-]$^{HN}\gamma$-PyPyPy-β-Pam-Resin. The Fmoc group was removed with (4:1) piperdine/DMF. A sample of resin was then cleaved by a single-step aminolysis reaction

0947-6539/99/0503-0976 $ 17.50+.50/0 *Chem. Eur. J.* **1999**, *5*, No. 3

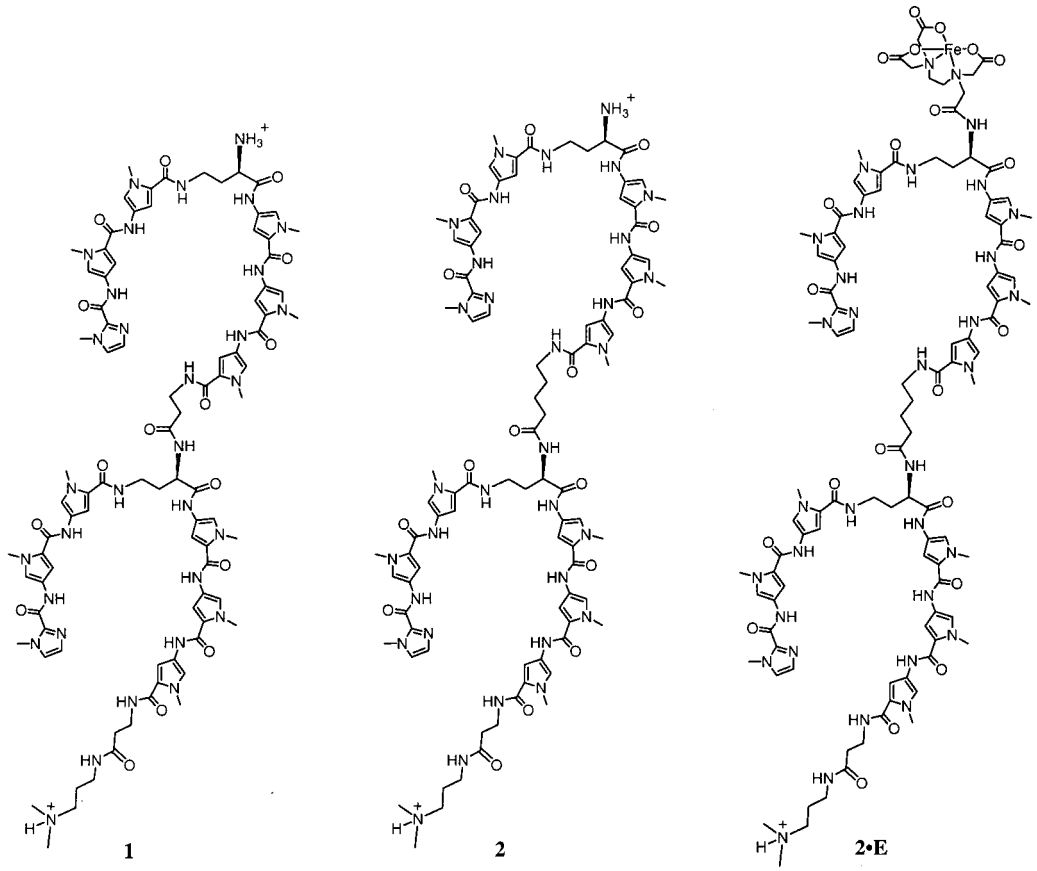

Figure 2. Structures of the 12-ring hairpin polyamides **1**, **2**, and **2-E** synthesized by solid phase methods.

with [(dimethylamino)propylamine 55 °C, 18 h], and the reaction mixture subsequently purified by reversed phase HPLC to provide **1** and **2**. For the synthesis of the EDTA-turn derivative **2-E**, a sample of **2** was treated with an excess of EDTA-dianhydride (DMSO/NMP, DIEA 55 °C, 30 min), and the remaining anhydride hydrolyzed (0.1M NaOH, 55 °C, 10 min). The polyamide **2-E** was then isolated by reverse phase HPLC. The dicationic twelve-ring tandem hairpins are soluble in aqueous solution at concentrations up to 1 mM. The solubility of the tandem hairpins is 10- to 100-fold greater than that found for extended or hairpin twelve-ring polyamides.

Binding-site size: MPE · Fe^{II} footprinting[13] on 3′- or 5′-^{32}P end-labeled 135-bp *Eco*RI/*Bsr*BI restriction fragments from the plasmid pDH11 reveals that polyamide **2**, at 100 pM concentration, binds to the designated 11-bp match site 5′-TGTTATTGTTA-3′ (25 mM Tris-acetate, 10 mM NaCl, pH 7.0 and 22 °C; Figures 4 and 5b, pp. 979, 980). Binding of the mismatch site 5′-TGT**C**ATTGT**C**A-3′ is only observed at much higher polyamide concentrations. The size of the asymmetrically 3′-shifted cleavage protection pattern for polyamide **2** at the designated match site 5′-TGTTATTGTTA-3′ is consistent with formation of the predicted hairpin-δ-hairpin · DNA complex.

Binding orientation: Affinity cleavage experiments[14] with **2-E**, which has an EDTA · Fe^{II} moiety appended to the γ-turn, were used to confirm polyamide binding orientation and stoichiometry. Affinity cleavage experiments were performed on the same 3′- or 5′-^{32}P end-labeled 135-bp DNA restriction fragment from the plasmid pDH11 (25 mM Tris-acetate, 10 mM NaCl, 100 μM/base pair calf thymus DNA, pH 7.0 and 22 °C). The observed cleavage pattern for **2-E** (Figures 5b and 5d) are 3′-shifted, consistent with minor groove occupancy. In the presence of 1 μM **2-E**, a single cleavage locus proximal to the 3′ side of the 5′-TGTTATTGTTA-3′ match sequence is revealed, consistent with formation of an oriented 1:1 hairpin-δ-hairpin · DNA complex.

Equilibrium association constants: Quantitative DNase I footprint titrations (10 mM Tris · HCl, 10 mM KCl, 10 mM $MgCl_2$ and 5 mM $CaCl_2$, pH 7.0 and 22 °C) were performed to determine the equilibrium association constants of **1** and **2** for the 10-, 11- and 12-bp match and mismatch sites (Table 1, Figure 4, p. 979). Polyamide **2** preferentially binds the 11-bp 5′-TGTTATTGTTA-3′ target sequence with, $K_a \geqslant 1 \times 10^{12}\,M^{-1}$. The corresponding 11-bp mismatch 5′-TGTCATTGTCA-3′ site is bound by **2** with $\geqslant$4500-fold lower affinity ($K_a = 2.2 \times 10^{8}\,M^{-1}$). Polyamide **2** binds the 10-bp site 5′-TGTTATGTTA-3′ ($K_a = 1.5 \times 10^{10}\,M^{-1}$) and the 12-bp site 5′-TGTTATATGTTA-3′ ($K_a = 1.0 \times 10^{9}\,M^{-1}$) with 70- and 1000-fold lower affinity, respectively. Polyamide **1** binds the 10-bp 5′-TGTTATGTTA-3′ site and 11-bp 5′-TGTTATTGTTA-3′ site with $K_a = 2 \times 10^{10}\,M^{-1}$, and also binds the 12-bp 5′-TGTTATATGTTA-3′ site with 16-fold lower affinity ($K_a = 9.0 \times 10^{9}\,M^{-1}$). The parent hairpin ImPyPy-

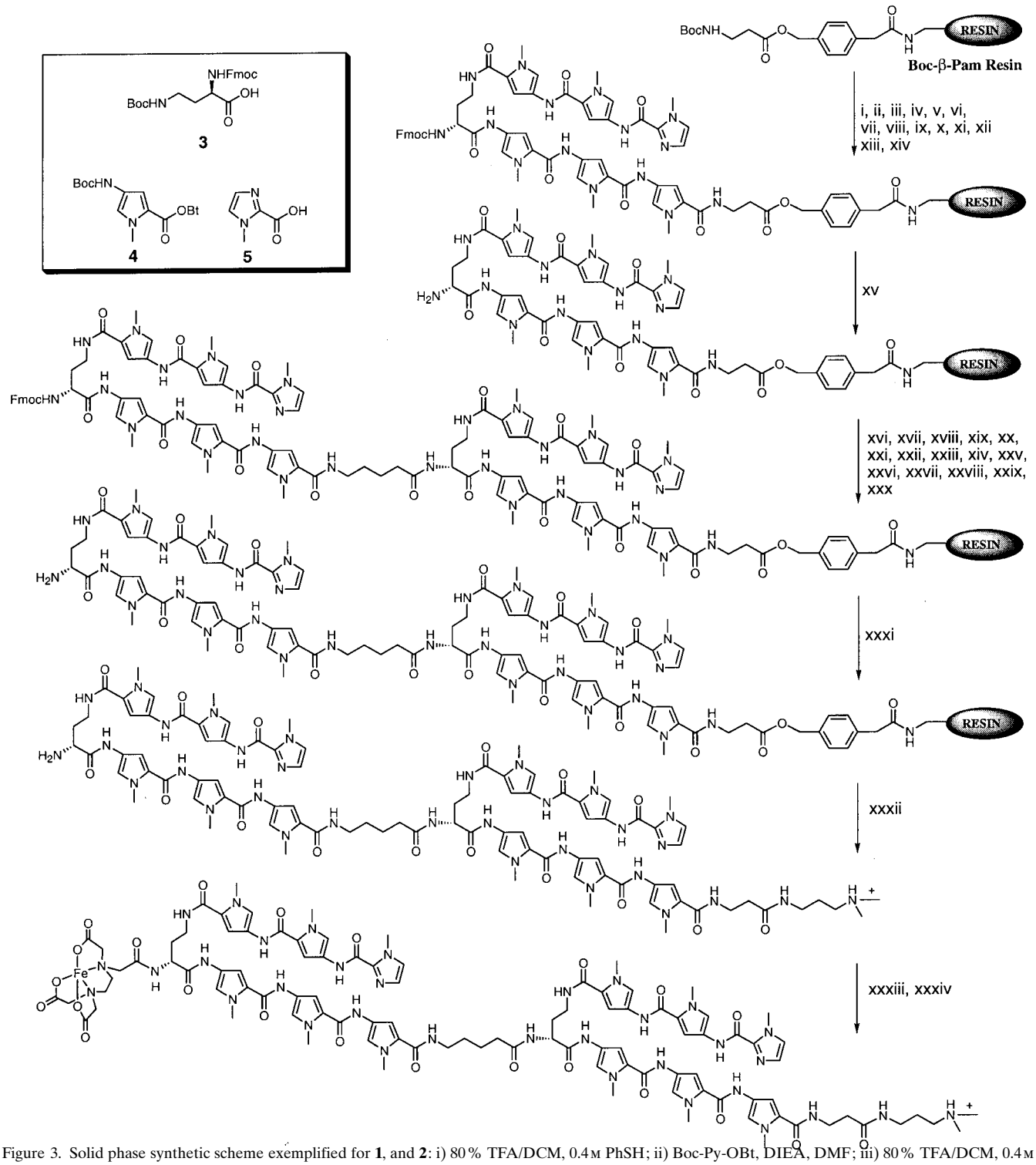

Figure 3. Solid phase synthetic scheme exemplified for **1**, and **2**: i) 80% TFA/DCM, 0.4 M PhSH; ii) Boc-Py-OBt, DIEA, DMF; iii) 80% TFA/DCM, 0.4 M PhSH; iv) Boc-Py-OBt, DIEA, DMF; v) 80% TFA/DCM, 0.4 M PhSH; vi) Boc-Py-OBt ,DIEA, DMF; vii) 80% TFA/DCM, 0.4 M PhSH; viii) Fmoc-α-Boc-γ-diaminobutyric acid (HBTU, DIEA); ix) 80% TFA/DCM, 0.4 M PhSH; x) Boc-Py-OBt, DIEA, DMF; xi) 80% TFA/DCM, 0.4 M PhSH; xii) Boc-Py-OBt, DIEA, DMF; xiii) 80% TFA/DCM, 0.4 M PhSH; xiv) imidazole-2-carboxylic acid (HBTU/DIEA); xv) 80% Piperdine:DMF (25 °C, 30 min); xvi) Boc-β-alanine (HOBT/DIEA) for **1;** Boc-valeric acid (HOBT/DIEA) for **2**; xvii) 80% TFA/DCM, 0.4 M PhSH; xviii) Boc-Py-OBt, DIEA, DMF; xix) 80% TFA/DCM, 0.4 M PhSH; xx) Boc-Py-OBt, DIEA, DMF; xxi) 80% TFA/DCM, 0.4 M PhSH; xxii) Boc-Py-OBt ,DIEA, DMF; xxiii) 80% TFA/DCM, 0.4 M PhSH; xxiv) Fmoc-α-Boc-γ-diaminobutyric acid (HBTU, DIEA); xxv) 80% TFA/DCM, 0.4 M PhSH; xxvi) Boc-Py-OBt, DIEA, DMF; xxvii) 80% TFA/DCM, 0.4 M PhSH; xxviii) Boc-Py-OBt, DIEA, DMF; xxix) 80% TFA/DCM, 0.4 M PhSH; xxx) imidazole-2-carboxylic acid (HBTU/DIEA); xxxi) 80% piperidine:DMF (25 °C, 30 min); xxxii) N-N-((dimethylamio)propyl)amine, 55 °C; xxxiii) EDTA-dianhydride, DMSO/NMP, DIEA (55 °C, 15 min); 0.1 M NaOH (55 °C, 10 min); xxxiv) $[Fe(NH_4)_2]SO_4 \cdot 6H_2O$; (Inset) Py, Im, and diaminobutyric acid monomers for solid phase synthesis: (*R*)-Fmoc-α-Boc-γ-diaminobutyric acid (**3-*R*),** Boc-pyrrole-OBt ester[12] (Boc-Py-OBt; **4**), and imidazole-2-Carboxylic acid[4a] (Im-OH; **5**).

0947-6539/99/0503-0978 $ 17.50+.50/0 *Chem. Eur. J.* **1999**, *5*, No. 3

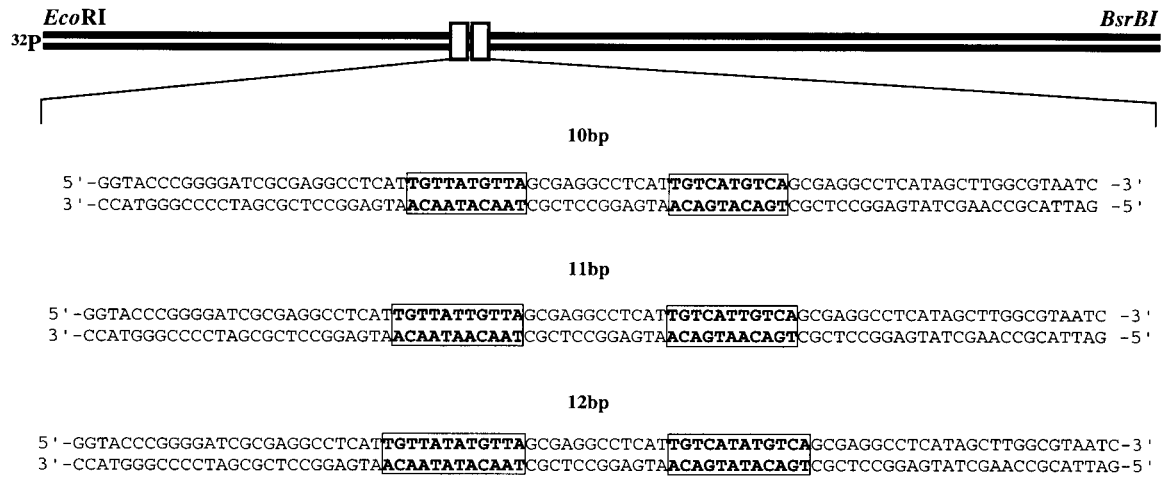

Figure 4. Sequence of the synthesized inserts from the pDH10, pDH11, and pDH12 plasmids containing 10-bp, 11-bp, and 12-bp match and mismatch target sites. Top: illustraion of the *Eco*RI/*Bsr*BI restriction fragments containing the *Bam*HI and *Hind*III inserts as indicated below. Only the boxed sites were analyzed by quantitative DNase I footprint titrations.

$(R)^{H_2N}\gamma$-PyPyPy-β-Dp was found to bind to the 5′-TGTTA-3′ match site with $K_a = 5 \times 10^9\,M^{-1}$.

Linker dependence: Site size preferences of polyamides **1** and **2** are modulated by the length of the turn-to-tail linker. Modeling indicated that β and δ linkers would provide sufficient length for recognition of either 10 or 11 base pairs, but would be too short to span the 12-bp binding site. Polyamide **2** displays optimal recognition of the 11-bp binding site, 5′-TGTTATTGTTA-3′, $K_a \geq 1 \times 10^{12}\,M^{-1}$. Replacing the δ linker in **2** with the two-carbon shorter β residue in **1** results in a reduction of affinity at the 11-bp site by >6-fold ($K_a = 1.5 \times 10^{10}\,M^{-1}$). The unfavorable binding affinities of **1** and **2** at the 12-bp site indicates that the covalent constraint of the linker subunit prevents alignment of hairpin subunits at this longer recognition sequence.

Conclusions

It might have been expected that tandem-hairpins would bind by a mechanism with one hairpin binding its 5-bp target site and the second hairpin providing nonspecific binding enhancement from van der Waals and electrostatic interactions. Surprisingly, a large affinity increase is observed only at the 11-bp target site, while affinity at isolated 5-bp hairpin sites does not increase substantially and in some cases decreases (Table 2, p. 981). These results indicate that a simple aliphatic 5-carbon linker is sufficient to provide for synergistic tandem-hairpin binding affinity and specificity. Although it is remarkable that simple aliphatic linkers provide six orders of magnitude enhancement in DNA-binding affinity, this still remains substantially lower than the nine order of magnitude enhancement predicted for a perfect linker. Therefore,

Table 1. Equilibrium association constants [M^{-1}].[a–c]

Polyamide	5'-TGTTATGTTA-3'	5'-TGTCATGTCA-3'	Specificity[d]
1	**2.0 x 10^{10}**	1.5 x 10^8	133
2	**1.5 x 10^{10}**	1.9 x 10^8	80
Polyamide	5'-TGTTATTGTTA-3'	5'-TGTCATTGTCA-3'	Specificity
1	**1.5 x 10^{10}**	2.7 x 10^8	55
2	**≥ 1 x 10^{12}**	2.2 x 10^8	≥ 4500
Polyamide	5'-TGTTATATGTTA-3'	5'-TGTCATATGTCA-3'	Specificity
1	**9.4 x 10^9**	3.1 x 10^7	30
2	**1.3 x 10^9**	2.5 x 10^7	52

[a] The reported association constants are the average values obrained from the three DNase I footprint titration experiments. [b] The assays were scarried out at 22 °C at pH 7.0 in the presence of 10 mM Tris-HCl, 10 mM KCl, 10 mM $MgCl_2$, and 5 mM $CaCl_2$. The 10-, 11-, and 12-bp sites are in capital letters. Match site association constants are shown in boldtype. [c] Half sites for tandem hairpin polyamide binding are underlined and mismatch bases are underlined in boldtype for all target sequences. [d] Specificity is caluclated as K_a(match)/K_a(mismatch).

  0947-6539/99/0503-0979 $ 17.50+.50/0

although the structural elements reported here for tail-to-turn coupling of hairpin polyamides expand the binding-site size targetable by the motif, the generality of the approach as well as second generation rigid linkers, will need to be explored and reported in due course.

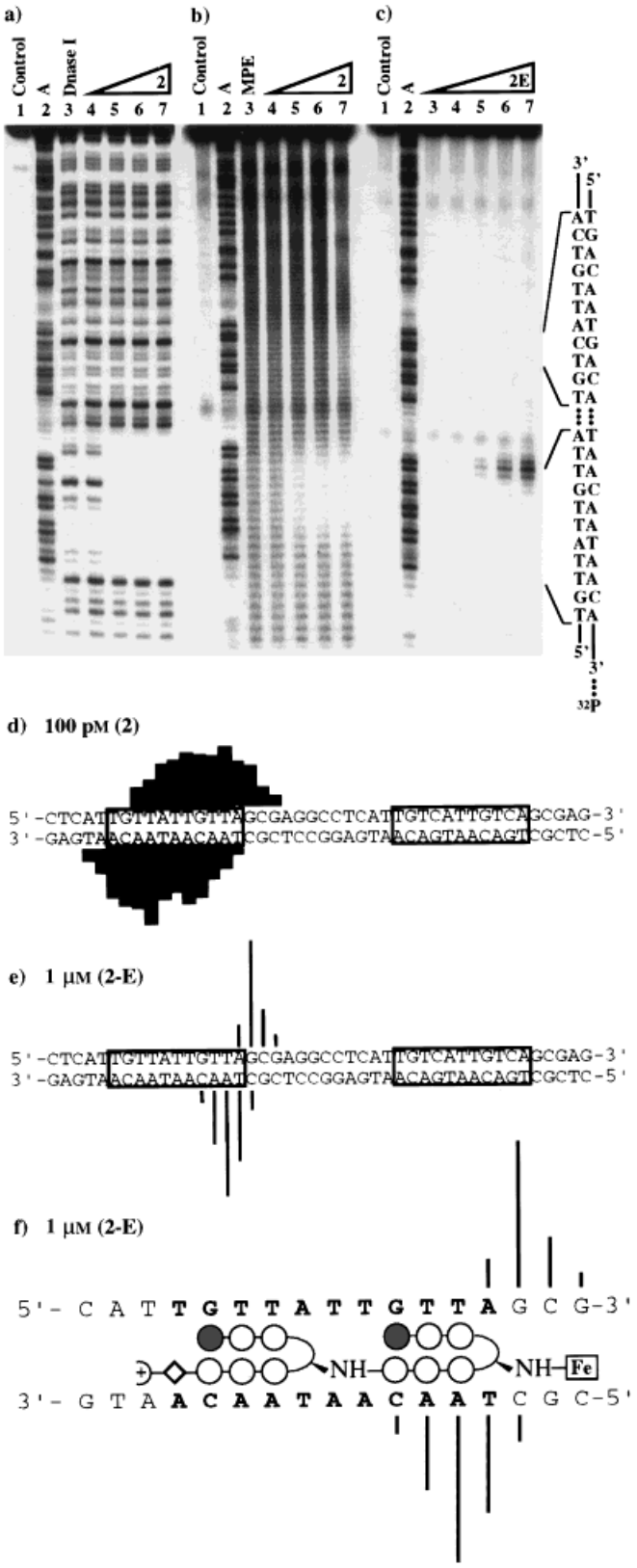

Figure 5. Footprinting experiments on the on a 3′-^{32}P-labeled 135-bp DNA restriction fragment derived from the plasmid pDH11. a) Quantitative Dnase I footprint titration experiment with **2**: lane 1, intact; lane 2, A reaction; lane 3, DNase I standard, lanes 4 – 7, 1 pM, 3 pM, 10 pM, and 30 pM. All reactions contain 10 kcpm restriction fragment, 10 mM Tris · HCl (pH 7.0), 10 mM KCl, 10 mM $MgCl_2$ and 5 mM $CaCl_2$. b) MPE · Fe^{II} footprinting of tandem-hairpin **2**: Lane 1, intact; lane 2, A reaction; lane 3, MPE · Fe^{II} standard; lanes 4 – 7; 10 pM, 100 pM, 1 nM, and 10 nM polyamide. c) affinity cleaving titration experiment with tandem-hairpin **2-E**: Lane 1, control reaction; lane 2, A reaction; lanes 3 – 7, 10 nM, 30 nM, 100 nM, 300 nM, and 1 μM polyamide. All lanes contain 15 kcpm 3′-radiolabeled DNA, 25 mM Tris-acetate buffer (pH 7.0), 10 mM NaCl, and 100 μM/base pair calf thymus DNA. 5′-TGTTATTGTTA-3′ and 5′-TGT**C**ATTGT**C**A-3′ sites are shown on the right side of the autoradiograms. d) MPE · Fe^{II} protection patterns for **2** at 100 pM concentration. Bar heights are proportional to the relative protection from cleavage at each band. e) Affinity cleaving pattern for **2-E** at 1 μM concentration. Bar heights are proportional to the relative cleavage intensities at each base pair. f) Ball and stick schematic of compound **2-E** · 11-bp 5′-TGTTATTGTTA-3′ complex showing the affinity cleaving data on the right side of the autoradiogram.

Experimental Section

General: Dicyclohexylcarbodiimide (DCC), Hydroxybenzotriazole (HOBt), 2-(1*H*-Benzotriazole-1-yl)-1,1,3,3-tetramethyluronium hexa-fluorophosphate (HBTU) and 0.2 mmol g^{-1} Boc-β-alanine-(4-carboxamidomethyl)-benzyl-ester-copoly(styrene-divinylbenzene) resin (Boc-β-Pam-Resin) was purchased from Peptides International (0.2 mmol g^{-1}) (*R*)-2-Fmoc-4-Boc-diaminobutyric acid, (*S*)-2-Fmoc-4-Boc-diaminobutyric acid, and (*R*)-2-amino-4-Boc-diaminobutyric acid were from Bachem. *N*,*N*-diisopropylethylamine (DIEA), *N*,*N*-dimethylformamide (DMF), *N*-methylpyrrolidone (NMP), DMSO/NMP, Acetic anhydride (Ac_2O), and 0.0002 M potassium cyanide/pyridine were purchased from Applied Biosystems. Dichloromethane (DCM) and triethylamine (TEA) were reagent grade from EM, thiophenol (PhSH), dimethylaminopropylamine (Dp), (*R*)-α-methoxy-α-(trifuoromethyl)phenylacetic acid ((*R*)MPTA), and (*S*)-α-methoxy-α-(trifouromethyl)phenylacetic acid [(*S*)MPTA] were from Aldrich, trifluoroacetic acid (TFA) Biograde from Halocarbon, phenol from Fisher, and ninhydrin from Pierce. All reagents were used without further purification. Quik-Sep polypropylene disposable filters were purchased from Isolab. A shaker for manual solid phase synthesis was obtained from St. John Associates. Screw-cap glass peptide synthesis reaction vessels (5 mL and 20 mL) with a #2 sintered glass frit were made as described by Kent.[16] ^{1}H NMR spectra were recorded on a General Electric-QE NMR spectrometer at 300 MHz with chemical shifts reported in parts per million relative to residual solvent. UV spectra were measured in water on a Hewlett – Packard Model 8452A diode array spectrophotometer. Optical rotations were recorded on a JASCO Dip 1000 Digital Polarimeter. Matrix-assisted, laser desorption/ionization time of flight mass spectrometry (MALDI-TOF) was performed at the Protein and Peptide Microanalytical Facility at the California Institute of Technology. HPLC analysis was performed on either a HP 1090M analytical HPLC or a Beckman Gold system using a RAINEN C_{18}, Microsorb MV, 5 μm, 300 × 4.6 mm reversed phase column in 0.1 % (wt v^{-1}) TFA with acetonitrile as eluent and a flow rate of 1.0 mL/ min, gradient elution 1.25 % acetonitrile min^{-1}. Preparatory reverse phase HPLC was performed on a Beckman HPLC with a Waters DeltaPak 25 × 100 mm, 100 μm C18 column equipped with a guard, 0.1 % (wt v^{-1}) TFA, 0.25 % acetonitrile min^{-1}. 18 MΩ water was obtained from a Millipore MilliQ water purification system, and all buffers were 0.2 μm filtered.

ImPyPy-(*R*)[ImPyPy-(*R*)^{H_2N}γ-PyPyPy-β-]^{HN}γ-PyPyPy-β-Dp (**1**): ImPyPy-(*R*)^{FmocHN}γ-PyPyPy-β-Pam-Resin was synthesized in a stepwise fashion by machine-assisted solid-phase methods from Boc-β-Pam-Resin (0.6 mmol g^{-1}).[12] (*R*)-2-Fmoc-4-Boc-diaminobutyric acid (0.7 mmol) was incorporated as previously described for Boc-γ-aminobutyric acid. ImPyPy-(*R*)^{FmocHN}γ-PyPyPy-β-Pam-Resin was placed in a glass 20 mL peptide synthesis vessel and treated with DMF (2 mL), followed by piperidine (8 mL) and agitated (22 °C, 30 min). ImPyPy-(*R*)^{H_2N}γ-PyPyPy-β-Pam-resin was isolated by filtration, and washed sequentially with an excess of DMF,

0947-6539/99/0503-0980 $ 17.50+.50/0 *Chem. Eur. J.* **1999**, *5*, No. 3

Table 2. Equilibrium association constants [M^{-1}] for binding the parent hairpin to 5-bp half sites and tandem hairpin at 11-bp mismatch sites.

Site	Hairpin Motif (H)	Tandem Hairpin Motif (T)	K_a(T)/K_a(H)	Specificity[d]
I	 $K_a = 3.8 \times 10^9\,M^{-1}$	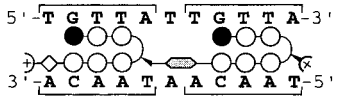 $K_a \geq 1.0 \times 10^{12}\,M^{-1}$	≥ 260	≥ 20,000
II	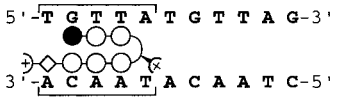 $K_a = 3.8 \times 10^9\,M^{-1}$	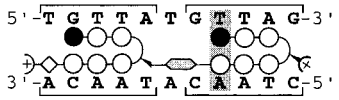 $K_a = 1.5 \times 10^{10}\,M^{-1}$	4	300
III	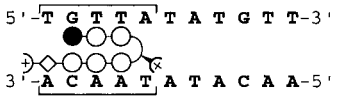 $K_a = 3.8 \times 10^9\,M^{-1}$	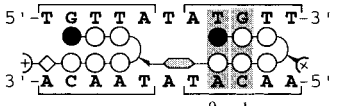 $K_a = 1.0 \times 10^9\,M^{-1}$	.26	20
IV	 $K_a = 3.5 \times 10^7\,M^{-1}$	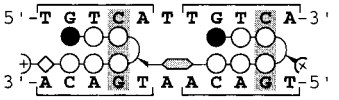 $K_a = 2.2 \times 10^8\,M^{-1}$	6	4.4
V	 $K_a \approx 3 \times 10^8\,M^{-1}$	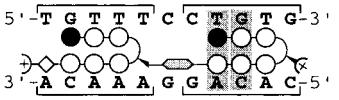 $K_a \approx 1 \times 10^8\,M^{-1}$	.33	2
VI	 $K_a \approx 1 \times 10^8\,M^{-1}$	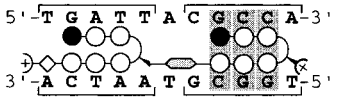 $K_a \approx 5 \times 10^7\,M^{-1}$	.5	1

[a] The reported association constants are the average values obrained from the three DNase I footprint titration experiments. [b] The assays were scarried out at 22 °C at pH 7.0 in the presence of 10 mM Tris-HCl, 10 mM KCl, 10 mM $MgCl_2$, and 5 mM $CaCl_2$. Mismatch base pairings are in the shaded regions and brackets enclose the binding site and half binding sites for the parent and tandem hairpins , respectively. [c] Sites V and VI were less accurately measured because they were located in the compresed region of the sequencing gel. [d] Specificity is caluclated as K_a(sites I – VI)/K_a(site VI).

DCM, MeOH, and ethyl ether and the amine-resin dried in vacuo. ImPyPy-(*R*)[ImPyPy-(*R*)^{FMocHN}γ-PyPyPy-β-]^{HN}γ-PyPyPy-β-Pam-Resin was then synthesized in a stepwise fashion by machine-assisted solid-phase methods from ImPyPy-(*R*)^{H_2N}γ-PyPyPy-β-Pam-resin (0.38 mmol g^{-1}[18]). ImPyPy-(*R*)[ImPyPy-(*R*)^{FMocHN}γ-PyPyPy-β-]^{HN}γ-PyPyPy-β-Pam-Resin was placed in a glass 20 mL peptide synthesis vessel and treated with DMF (2 mL), followed by piperidine (8 mL) and agitated (22 °C, 30 min). ImPyPy-(*R*)[ImPyPy-(*R*)^{H_2N}γ-PyPyPy-β-]^{HN}γ-PyPyPy-β-Pam-Resin was isolated by filtration and washed sequentially with an excess of DMF, DCM, MeOH, and ethyl ether, and the amine-resin dried in vacuo. A sample of ImPyPy-(*R*)[ImPyPy-(*R*)^{H_2N}γ-PyPyPy-β-]^{HN}γ-PyPyPy-β-Pam-Resin (240 mg, 0.29 mmol g^{-1}[19]) was treated with neat dimethylaminopropylamine (2 mL) and heated (55 °C) with periodic agitation for 16 h. The reaction mixture was then filtered to remove resin, TFA was added [0.1 % (wt v^{-1}), 6 mL], and the resulting solution purified by reversed phase HPLC. Polyamide **1** was recovered upon lyophilization of the appropriate fractions as a white powder (28 mg, 22 % recovery). $[\alpha]_D^{20} = +14.6$ ($c = 0.05$ in H_2O); UV (H_2O): $\lambda_{max} = 246$, 306 (100000); ^{1}H NMR (300 MHz, [D_6]DMSO, 20 °C): $\delta = 10.54$ (s, 1H; aromatic NH), 10.45 (s, 1H; aromatic NH), 10.44 (s, 1H; aromatic NH), 10.02 (s, 1H; aromatic NH), 9.95 (s, 1H; aromatic NH), 9.92 (s, 1H; aromatic NH), 9.90 (d, 2H; aromatic NH), 9.86 (d, 2H; aromatic NH), 9.2 (br s, 1H; CF_3COOH), 8.25 (m, 4H; aliphatic NH, NH_3), 8.11 (d, 1H; $J = 8.5$ Hz, aliphatic NH), 8.04 (m, 4H, aliphatic NH), 7.37 (s, 2H; CH), 7.25 (m, 2H; CH), 7.22 (d, 1H; CH), 7.18 (m, 2H; CH), 7.16 (m, 3H; CH), 7.12 (m, 4H; CH), 7.02 (m, 4H; CH), 6.95 (d, $J = 1.6$ Hz, 1H; CH), 6.91 (d, $J = 1.5$ Hz, 1H; CH), 6.88 (d, $J = 1.3$ Hz, 1H; CH), 6.85 (m, 3H; CH), 5.32 (t, 1H; aliphatic CH), 4.45 (m, 1H, aliphatic CH), 3.96 (s, 6H; NCH_3), 3.83 (s, 3H; NCH_3), 3.80 (s, 18H; NCH_3), 3.79 (s, 3H; NCH_3), 3.76 (s, 3H; NCH_3), 3.39 (m, 4H; CH_2), 3.28 (m, 2H; CH_2), 3.15 (m, 4H; CH_2), 3.07 (m, 2H; CH_2), 2.97 (m, 2H; CH_2), 2.70 (d, 6H; $N(CH_3)_2$), 2.32 (m, 2H; CH_2), 1.93 (m, 2H; CH_2), 1.71 (m, 2H; CH_2), 1.47 (m, 2H; CH_2), 1.20 (m, 4H; CH_2); MALDI-TOF-MS (monoisotopic): m/z: 1881.9 [$M^+ - H$]; calcd $C_{89}H_{109}N_{32}O_{16}$ 1881.9

ImPyPy-(*R*)[ImPyPy-(*R*)^{H_2N}γ-PyPyPy-δ-]^{HN}γ-PyPyPy-β-Dp (**2**): ImPyPy-(*R*)[ImPyPy-(*R*)^{H_2N}γ-PyPyPy-δ-]^{HN}γ-PyPyPy-β-Pam-Resin was prepared as described for ImPyPy-(*R*)[ImPyPy-(*R*)^{H_2N}γ-PyPyPy-β-]^{HN}γ-PyPyPy-β-Pam-Resin. A sample of ImPyPy-(*R*)[ImPyPy-(*R*)^{H_2N}γ-PyPyPy-δ-]^{HN}γ-PyPyPy-β-Pam-Resin (240 mg, 0.29 mmol g^{-1}[18]) was treated with neat dimethylaminopropylamine (2 mL) and heated (55 °C) with periodic agitation for 16 h. The reaction mixture was then filtered to remove resin, TFA was added [0.1 % (wt v^{-1}); 6 mL], and the resulting solution purified by reversed phase HPLC. Polyamide **2** was recovered upon lyophilization of the appropriate fractions as a white powder (32 mg, 25 % recovery). $[\alpha]_D^{20} = +14.6$ ($c = 0.05$ in H_2O); UV (H_2O) $\lambda_{max} = 246$, 306 (100000); ^{1}H NMR (300 MHz, [D_6]DMSO, 20 °C): $\delta = 10.54$ (s, 1H; aromatic NH), 10.45 (s, 1H; aromatic NH), 10.44 (s, 1H; aromatic NH), 10.02 (s, 1H; aromatic NH), 9.95 (s, 1H; aromatic NH), 9.92 (s, 1H; aromatic NH), 9.90 (d, 2H; aromatic NH), 9.86 (d, 2H; aromatic NH), 9.2 (br s, 1H; CF_3COOH), 8.25 (m, 4H; aliphatic NH, NH_3), 8.11 (d, $J = 8.5$ Hz, 1H;

aliphatic NH), 8.04 (m, 4H, aliphatic NH), 7.37 (s, 2H; CH), 7.25 (m, 2H; CH), 7.22 (d, 1H; CH), 7.18 (m, 2H; CH), 7.16 (m, 3H; CH), 7.12 (m, 4H; CH), 7.02 (m, 4H; CH), 6.95 (d, $J = 1.6$ Hz, 1H; CH), 6.91 (d, $J = 1.5$ Hz, 1H; CH), 6.88 (d, $J = 1.3$ Hz, 1H; CH), 6.85 (m, 3H; CH), 5.32 (t, 1H; aliphatic CH), 4.45 (m, 1H, aliphatic CH), 3.96 (s, 6H; NCH_3), 3.83 (s, 3H; NCH_3), 3.80 (s, 18H; NCH_3), 3.79 (s, 3H; NCH_3), 3.76 (s, 3H; NCH_3), 3.39 (m, 4H; CH_2), 3.28 (m, 2H; CH_2), 3.15 (m, 4H; CH_2), 3.07 (m, 2H; CH_2), 2.97 (m, 2H; CH_2), 2.70 (d, 6H; $N(CH_3)_2$), 2.32 (m, 2H; CH_2), 1.93 (m, 2H; CH_2), 1.71 (m, 2H; CH_2), 1.47 (m, 2H; CH_2), 1.20 (m, 4H; CH_2); MALDI-TOF-MS (monoisotopic): m/z: 1910.2 $[M^+ - H]$; calcd $C_{91}H_{113}N_{32}O_{16}$ 1909.9.

ImPyPy-(*R*)[ImPyPy-(*R*)^{EDTA}γ-PyPyPy-δ-]^{HN}γ-PyPyPy-β-Dp (2-E): Excess EDTA-dianhydride (50 mg) was dissolved in DMSO/NMP (1 mL) and DIEA (1 mL) by heating at 55 °C for 5 min The dianhydride solution was added to ImPyPy-(*R*)[ImPyPy-(*R*)^{H_2N}γ-PyPyPy-δ-]^{HN}γ-PyPyPy-β-Dp (10 mg, 5 μmol) dissolved in DMSO (750 μL). The mixture was heated (55 °C, 25 min) and the remaining EDTA-anhydride hydrolyzed (0.1 M NaOH, 3 mL, 55 °C, 10 min). Aqueous TFA (0.1 % wt v^{-1}) was added to adjust the total volume to 8 mL, and the solution was purified directly by reversed phase HPLC to provide **2-E** as a white powder upon lyophilization of the appropriate fractions (2 mg, 20 % recovery). MALDI-TOF-MS (monoisotopic): m/z: 2184.3 $[M^+ - H]$: calcd $C_{101}H_{127}N_{34}O_{23}$ 2184.0.

DNA reagents and materials: Enzymes were purchased from Boehringer-Mannheim and used with their supplied buffers. Deoxyadenosine and thymidine 5′-[α-^{32}P] triphosphates were obtained from Amersham, deoxyadenosine 5′-[γ-^{32}P]triphosphate was purchased from I.C.N. Sonicated, and deproteinized calf thymus DNA was acquired from Pharmacia. RNase free water was obtained from USB and used for all footprinting reactions. All other reagents and materials were used as received. All DNA manipulations were performed according to standard protocols.[17]

Construction of plasmid DNA: The plasmids pDH10, pDH11, and pDH12 were constructed by hybridization of the inserts listed in Figure 4. Each hybridized insert was ligated individually into linearized pUC19 *Bam*HI/*Hind*III plasmid with T4 DNA ligase. The resultant constructs were used to transform Top10F′ OneShot competent cells from Invitrogen. Ampicillin-resistant white colonies were selected from 25 mL Luria-Bertani medium-agar plates containing 50 μg mL^{-1} ampicillin and treated with XGAL and IPTG solutions. Large-scale plasmid purification was performed with Qiagen Maxi purification kits. Dideoxy sequencing was used to verify the presence of the desired insert. Concentration of the prepared plasmid was determined at 260 nm from the relationship of 1 OD unit = 50 μg mL^{-1} duplex DNA.

Preparation of 3′- and 5′-end-labeled restriction fragments: The plasmids pDH(11 – 12) were linearized with *Eco*RI and *Bsr*BI, and were then treated with the Sequenase enzyme, deoxyadenosine 5′-[α-^{32}P]triphosphate, and thymidine 5′-[α-^{32}P]triphosphate for 3′ labeling. Alternatively, these plasmids were linearized with *Eco*RI, treated with calf alkaline phosphatase, and then 5′ labeled with T4 polynucleotide kinase and deoxyadenosine 5′-[γ-^{32}P]triphosphate. The 5′ labeled fragment was then digested with *Bsr*BI. The labeled fragment (3′ or 5′) was loaded onto a 6 % nondenaturing polyacrylamide gel, and the desired bp band was visualized by autoradiography and isolated. Chemical sequencing reactions were performed according to published methods.[19]

MPE · Fe^{II} footprinting:[13] All reactions were carried out in a volume of 40 μL. A polyamide stock solution or water (for reference lanes) was added to an assay buffer where the final concentrations were: 25 mM Tris-acetate buffer (pH 7.0), 10 mM NaCl, 100 μM/base pair calf thymus DNA, and 30 kcpm 3′- or 5′-radiolabeled DNA. The solutions were allowed to equilibrate for 4 hours. A fresh 50 μM MPE · Fe^{II} solution was prepared from 100 μL of a 100 μM MPE solution and 100 μL of a 100 μM ferrous ammonium sulfate ($[Fe(NH_4)_2(SO_4)_2] \cdot 6H_2O$) solution. MPE · Fe^{II} solution (5 μM) was added to the equilibrated DNA, and the reactions were allowed to equilibrate for 5 minutes. Cleavage was initiated by the addition of dithiothreitol (5 mM) and allowed to proceed for 14 min. Reactions were stopped by ethanol precipitation, resuspended in 100 mM tris-borate-EDTA/80 % formamide loading buffer, denatured at 85 °C for 6 min, and a 5 μL sample (~15 kcpm) was immediately loaded onto an 8 % denaturing polyacrylamide gel (5 % crosslink, 7 M urea) at 2000 V.

Affinity cleaving:[14] All reactions were carried out in a volume of 40 μL. A polyamide stock solution or water (for reference lanes) was added to an assay buffer where the final concentrations were: 25 mM Tris-acetate buffer (pH 7.0), 20 mM NaCl, 100 μM/base pair calf thymus DNA, and 20 kcpm 3′- or 5′-radiolabeled DNA. The solutions were allowed to equilibrate for 8 hours. A fresh solution of ferrous ammonium sulfate ($[Fe(NH_4)_2(SO_4)_2] \cdot 6H_2O$; 10 μM) was added to the equilibrated DNA, and the reactions were allowed to equilibrate for 15 min. Cleavage was initiated by the addition of dithiothreitol (10 mM) and allowed to proceed for 30 min. Reactions were stopped by ethanol precipitation, resuspended in 100 mM trisborate-EDTA/80 % formamide loading buffer, denatured at 85 °C for 6 min, and the entire sample was immediately loaded onto an 8 % denaturing polyacrylamide gel (5 % crosslink, 7 M urea) at 2000 V.

DNase I footprinting:[15] All reactions were carried out in a volume of 400 μL. We note explicitly that no carrier DNA was used in these reactions until after DNase I cleavage. A polyamide stock solution or water (for reference lanes) was added to an assay buffer in which the final concentrations were: 10 mM Tris · HCl buffer (pH 7.0), 10 mM KCl, 10 mM $MgCl_2$, 5 mM $CaCl_2$, and 30 kcpm 3′-radiolabeled DNA. The solutions were allowed to equilibrate for a minimum of 12 hours at 22 °C. Cleavage was initiated by the addition of 10 μL of a DNase I stock solution (diluted with 1 mM DTT to give a stock concentration of 1.875 u mL^{-1}) and was allowed to proceed for 7 min at 22 °C. The reactions were stopped by adding 50 μL of a solution containing NaCl (2.25 M), EDTA (150 mM), glycogen (0.6 mg mL^{-1}), and base-pair calf thymus DNA (30 μM), and then ethanol was added to precipitate the products. The cleavage products were resuspended in 100 mM trisborate-EDTA/80 % formamide loading buffer, denatured at 85 °C for 6 min, and immediately loaded onto an 8 % denaturing polyacrylamide gel (5 % crosslink, 7 M urea) at 2000 V for 1 hour. The gels were dried under vacuum at 80 °C, then quantitated by the use of storage phosphor technology. Equilibrium association constants were determined as previously described.[11a] The data were analyzed by performing volume integrations of the 5′-TGTTAxTGTTA-3′ and 5′-TGACAxTGACA-3 sites and a reference site. The apparent DNA target site saturation, θ_{app}, was calculated for each concentration of polyamide from Equation (1), in which I_{tot} and I_{ref} are the integrated volumes of the target and reference sites, respectively, and I^o_{tot} band I^o_{ref} correspond to those values for a DNase I control lane to which no polyamide has been added. The ($[L]_{tot}$, θ_{app}) data points were fitted to a Langmuir binding isotherm [Eq. (2), $n = 1$ for polyamides **1** and **2**] by minimizing the difference between $\theta_{app.}$ and θ_{fit}, by use of the modified Hill equation [Eq. (2)]. In Equation (2) $[L]_{tot}$ corresponds to the total polyamide concentration, K_a corresponds to the equilibrium association constant, and θ_{min} and θ_{max} represent the experimentally determined site saturation values when the site is unoccupied or saturated, respectively. Data were fit by means of a nonlinear least-squares fitting procedure of KaleidaGraph software (version 2.1, Abelbeck software) with K_a, $\theta_{max,}$ and θ_{min} as the adjustable parameters. All acceptable fits had a correlation coefficient of $R > 0.97$. At least three sets of acceptable data were used in determining each association constant. All lanes from each gel were used unless visual inspection revealed a data point to be obviously flawed relative to neighboring points. The data were normalized using the Equation (3).

$$\theta_{app} = 1 - \frac{I_{tot}/I_{ref}}{I^o_{tot}/I^o_{ref}} \quad (1)$$

$$\theta_{fit} = \theta_{min} + (\theta_{max} - \theta_{min}) \frac{K^n_a[L]^n_{tot}}{1} + K^n_a[L]^n_{tot} \quad (2)$$

$$\theta_{norm} = \frac{\theta_{app} - \theta_{min}}{\theta_{max} - \theta_{min}} \quad (3)$$

Quantitation by storage phosphor technology autoradiography: Photostimulable storage phosphor imaging plates (Kodak Storage Phosphor Screen S0230 obtained from Molecular Dynamics) were pressed flat against gel samples and exposed in the dark at 22 °C for 12 – 20 h. A Molecular Dynamics 400S PhosphorImager was used to obtain all data from the storage screens. The data were analyzed by performing volume integrations of all bands with use of the ImageQuant version 3.2.

Acknowledgments

We are grateful to the National Institutes of Health (GM-27681) for research support, the National Institutes of Health for a research service award to D.M.H., and the Howard Hughes Medical Institute for a predoctoral fellowship to E.E.B. We thank G.M. Hathaway for MALDI-TOF mass spectrometry.

0947-6539/99/0503-0982 $ 17.50+.50/0 *Chem. Eur. J.* **1999**, *5*, No. 3

[1] a) J. M. Gottesfeld, L. Nealy, J. W. Trauger, E. E. Baird, P. B. Dervan, *Nature* **1997**, *387*, 202; b) L. A. Dickinson, R. J. Gulizia, J. W. Trauger, E. E. Baird, D. E. Mosier, J. M. Gottesfeld, P. B. Dervan *Proc. Natl. Acad. Sci. USA* **1998**, *95*, 12890.

[2] a) J. W. Trauger, E. E. Baird, P. B. Dervan, *Nature* **1996**, *382*, 559; b) S. E. Swalley, E. E. Baird, P. B. Dervan, *J. Am. Chem. Soc.* **1997**, *119*, 6953; c) J. M. Turner, E. E. Baird, P. B. Dervan, *J. Am. Chem. Soc.* **1997**, *119*, 7636; d) J. W. Trauger, E. E. Baird, P. B. Dervan, *Angew. Chem.* **1998**, *37*, 1421; e) J. M. Turner, S. E. Swalley, E. E. Baird, P. B. Dervan, *J. Am. Chem. Soc.* **1998**, *120*, 6219.

[3] a) S. White, J. W. Szewczyk, J. M. Turner, E. E. Baird, P. B. Dervan, *Nature* **1998**, *391*, 468; b) C. L. Kielkopf, S. White, J. W. Szewczyk, J. M. Turner, E. E. Baird, P. B. Dervan, D. C. Rees *Science* **1998**, *282*, 111.

[4] a) W. S. Wade, M. Mrksich, P. B. Dervan, *J. Am. Chem. Soc.* **1992**, *114*, 8783; b) M. Mrksich, W. S. Wade, T. J. Dwyer, B. H. Geierstanger, D. E. Wemmer, P. B. Dervan, *Proc. Natl. Acad. Sci., USA* **1992**, *89*, 7586; c) W. S. Wade, M. Mrksich, P. B. Dervan, *Biochemistry* **1993**, *32*, 11385; d) M. Mrksich, P. B. Dervan, *J. Am. Chem. Soc.* **1993**, *115*, 2572; e) B. H. Geierstanger, M. Mrksich, P. B. Dervan, D. E. Wemmer, *Science* **1994**, *266*, 646; f) S. White, E. E. Baird, P. B. Dervan, *J. Am. Chem. Soc.* **1997,** *119*, 8756.

[5] a) J. G. Pelton, D. E. Wemmer, *Proc. Natl. Acad. Sci. USA* **1989**, *86*, 5723; b) J. G. Pelton, D. E. Wemmer, *J. Am. Chem. Soc.* **1990**, *112*, 1393; c) S. White, E. E. Baird, P. B. Dervan, *Biochemistry* **1996**, *35*, 12532; d) X. Chen, M. Sundaralingham Ramakrishnan, *J. Mol. Biol.* **1997**, *267*, 1157.

[6] C. L. Kielkopf, E. E. Baird, P. B. Dervan, D. C. Rees *Nature Struct. Biol.* **1998**, *5*, 104.

[7] a) J. J. Kelly, E. E. Baird, P. B. Dervan, *Proc. Natl. Acad. Sci. USA* **1996**, *93*, 6981; b) J. W. Trauger, E. E. Baird, M. Mrksich, P. B. Dervan, *J. Am. Chem. Soc.* **1996**, *118*, 6160; c) B. H. Geierstanger, M. Mrksich, P. B. Dervan, D. E. Wemmer, *Nature Struct. Biol.* **1996**, *3*, 321; d) S. E. Swalley, E. E. Baird, P. B. Dervan, *Chem. Eur. J.* **1997**, *3*, 1608; e) J. W. Trauger, E. E. Baird, P. B. Dervan, *J. Am. Chem*. **1998**, *120*, 3534.

[8] a) M. Mrksich, P. B. Dervan, *J. Am. Chem. Soc.* **1993**, *115*, 9892; b) T. J. Dwyer, B. H. Geierstanger, M. Mrksich, P. B. Dervan, D. E. Wemmer, *J. Am. Chem. Soc.* **1993**, *115*, 9900; c) M. Mrksich, P. B. Dervan, *J. Am. Chem. Soc.* **1994**, *116*, 3663; d) Y. H. Chen, J. W. Lown, *J. Am. Chem. Soc.* **1994**, *116*, 6995; e) N. H. Alsaid, J. W. Lown, *Tett. Lett.* **1994**, *35*, 7577; f) N. H. Alsaid, J. W. Lown, *Synth. Comm.* **1995**, *25*, 1059; g) Y. H. Chen, J. W. Lown, *Biophys. J.* **1995**, *68*, 2041; h) Y. H. Chen, J. X. Liu, J. W. Lown, *Bioorg. Med. Chem. Lett.* **1995**, *5*, 2223; i) Y. H. Chen, Y. W. Yang, J. W. Lown, *J. Biomol. Struct. Dyn.* **1996**, *14*, 341; j) M. P. Singh, W. A. Wylie, J. W. Lown, *Magn. Res. Chem.* **1996**, *34*, S55; k) W. A. Greenberg, E. E. Baird, P. B. Dervan, *Chem. Eur. J.* **1998**, *4*, 796.

[9] a) M. Mrksich, M. E. Parks, P. B. Dervan, *J. Am. Chem. Soc.* **1994**, *116*, 7983; b) M. E. Parks, E. E. Baird, P. B. Dervan, *J. Am. Chem. Soc.* **1996**, *118*, 6147; c) M. E. Parks, E. E. Baird, P. B. Dervan, *J. Am. Chem. Soc.* **1996**, *118*, 6153; d) J. W. Trauger, E. E. Baird, P. B. Dervan, *Chem. Biol.* **1996**, *3*, 369; e) S. E. Swalley, E. E. Baird, P. B. Dervan, *J. Am. Chem. Soc.* **1996**, *118*, 8198; f) D. S. Pilch, N. A. Pokar, C. A. Gelfand, S. M. Law, K. J. Breslauer, E. E. Baird, P. B. Dervan, *Proc. Natl. Acad. Sci. USA* **1996**, *93*, 8306; g) R. P. L. de Claire, B. H. Geierstanger M. Mrksich, P. B. Dervan, D. E. Wemmer, *J. Am. Chem. Soc.* **1997**, *119*, 7909; h) S. White, E. E. Baird, P. B. Dervan, *J. Am. Chem. Soc.* **1997**, *119*, 8756; i) S. White, E. E. Baird, P. B. Dervan, *Chem Biol.* **1997**, *4*, 569.

[10] D. H. Herman, E. E. Baird, P. B. Dervan, *J. Am. Chem. Soc.* **1998**, *120*, 1382.

[11] For a review, see: D. E. Wemmer and P. B. Dervan, *Curr. Opin. Struct. Biol.* **1997**, *7*, 355.

[12] E. E. Baird, P. B. Dervan, *J. Am. Chem. Soc.* **1996**, *118*, 6141.

[13] a) M. W. Van Dyke, R. P. Hertzberg, P. B. Dervan, *Proc. Natl. Acad. Sci. U.S.A.* **1982**, *79*, 5470; b) M. W. Van Dyke, P. B. Dervan, *Science* **1984**, *225*, 1122.

[14] a) J. S. Taylor, P. G. Schultz, P. B. Dervan, *Tetrahedron* **1984**, *40*, 457; b) P. B. Dervan, *Science* **1986**, *232*, 464.

[15] a) M. Brenowitz, D. F. Senear, M. A. Shea, G. K. Ackers, *Methods Enzymol*. **1986**, *130*, 132; b) M. Brenowitz, D. F. Senear, M. A. Shea, G. K. Ackers, *Proc. Natl. Acad. Sci. USA* **1986**, *83*, 8462; c) D. F. Senear, M. Brenowitz, M. A. Shea, G. K. Ackers, *Biochemistry* **1986**, *25*, 7344.

[16] S. B. H. Kent, *Annu. Rev. Biochem.* **1988**, *57*, 957.

[17] J. Sambrook, E. F. Fritsch, T. Maniatis, *Molecular Cloning*, Cold Spring Harbor Laboratory, Cold Spring Harbor, NY, **1989**.

[18] Resin substitution can be calculated as $L_{new}(\mathrm{mmol\,g^{-1}}) = L_{old}/(1 + L_{old}(W_{new} - W_{old}) \times 10^{-3})$, in which L is the loading (mmol of amine per gram of resin), and W is the weight ($\mathrm{g\,mol^{-1}}$) of the growing polyamide attached to the resin. see: K. Barlos, O. Chatzi, D. Gatos, G. Stravropoulos, *Int. J. Peptide Protein Res.* **1991**, *37*, 513.

[19] a) B. L. Iverson, P. B. Dervan, *Nucl. Acids Res.* **1987**, *15*, 7823; b) A. M. Maxam, W. S. Gilbert, *Methods Enzymol.* **1980**, *65*, 499.

Received: August 31, 1998 [F1328]